

Tracer-diffusion study of Cu^+ diffusion in CuBr

Jens-Erik Jørgensen

Department of Chemistry, Aarhus University, DK-8000 Århus C, Denmark

J. X. M. Z. Johansson and K. Sköld

Institute for Neutron Research, Uppsala University, S-61182 Nyköping, Sweden

(Received 14 March 1995)

Diffusion coefficients for Cu^+ diffusion in the γ , β , and α phases of CuBr have been measured with an *in situ* tracer diffusion technique. The diffusion in the γ and β phases obeys an Arrhenius law within measured temperature ranges and the activation energies were found to be 1.21(7) and 0.324(1) eV, respectively. A comparison of diffusion coefficients measured by the *in situ* tracer diffusion technique and diffusion coefficients calculated from conductivity data suggests that a noncharge carrying diffusion mechanism is operational in the copper halides.

I. INTRODUCTION

Fast ionic conduction in the copper halides CuX ($X = \text{Cl}, \text{Br}, \text{I}$) has been studied for several years. These compounds are of interest both from a scientific and from a technological point of view because they form a cheaper alternative to the silver containing fast ionic conductors. The copper halides form a series of isostructural compounds exhibiting several interesting properties such as sequences of structural phase transitions accompanied by large increases in the ionic conductivity. All three compounds have the cubic zinc-blende structure in their low-temperature γ phases. Their β phases are hexagonal and the fast ionic conducting α phases are cubic. The structure of α -CuBr is closely related to the α -AgI structure in which the iodine ions form a body-centered-cubic lattice. It has been proposed that α -CuI has the zinc-blende structure in which the iodine ions are arranged on a face-centered-cubic lattice. However, a recent neutron-diffraction study has shown that the Cu^+ ions in α -CuI are randomly distributed over all the tetrahedral sites.^{1,2} Only CuBr and CuI transform to the α phase, while in the case of CuCl melting takes place before the structure transforms to the α phase. In the case of CuBr the γ - β and β - α transitions take place at 658 and 743 K, respectively.³

The copper halides form a useful series of compounds for studies of the relationship between crystal structure, chemical bonding, lattice dynamics, and fast ionic conduction. The Cu^+ ion is very favorable for diffusion in the solid state because of its high polarizability and the series of anions Cl^- , Br^- , and I^- exhibit an increasing polarizability as well as decreasing electronegativity. The degree of covalency therefore increases along this series and copper iodide would be expected to have the highest ionic conductivity for a given crystal structure. However, a comparison of measured conductivities shows that the ionic conductivity decreases by going from CuCl to CuI at the upper end of the temperature interval in which the γ phases are stable.⁴ The large change in the ratio of cation and anion masses occurring by going from CuCl to

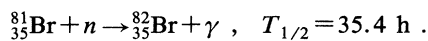
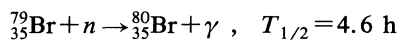
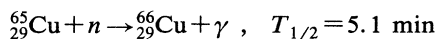
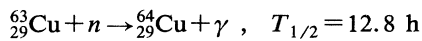
CuI is also of importance for the dynamics of these compounds.

Measurements of diffusion coefficients are important for the understanding of the physical properties of fast ionic conductors, and we have therefore performed a series of *in situ* tracer-diffusion studies of Cu^+ diffusion in the copper halides. The radioactive Cu^+ tracer ions in this method are generated within a thin slice in the sample material itself by neutron irradiation. The values for the diffusion coefficients obtained from these studies will be used for an evaluation of the usefulness of the interatomic pair potentials used for molecular-dynamics simulations of the static and dynamic properties of these compounds. The aim of these studies is to study and compare the pair potentials of the copper halides in the solid phases as well as in the liquid state. Diffusion in CuI has previously been studied by an *in situ* tracer method as well as being simulated by molecular dynamics.^{5,6} Recently we have performed studies of Cu^+ diffusion in β phase CuI and γ and β phase CuCl.^{7,8} Schäfergen and Richtering have performed a conventional tracer-diffusion study of γ -CuBr.⁹ In this paper we present the results of *in situ* tracer-diffusion studies of the γ , β , and α phases of CuBr and these results are compared with the previous diffusion studies as well as with conductivity measurements.

II. EXPERIMENT

The experimental setup used for *in situ* tracer-diffusion measurements has been described earlier in connection with measurements on CuCl and CuI.^{7,8} The CuBr sample was made from CuBr powder (BDH Chemicals Ltd., Product No. 27853) melted together in a Pyrex ampoule. X-ray diffraction showed that the sample contained no impurity phases. No chemical analysis was done. The sample used for *in situ* tracer-diffusion measurements is enclosed in a cylindrical Pyrex ampoule and the radioactive tracer ions are generated in a thin slice located in the middle of the sample by neutron irradiation. The neutrons penetrate into the sample through a 1 to 2 mm wide

slit in the boron nitride shield in which the sample is located during irradiation. The activated rod-shaped sample is heated to the desired temperature and the time evolution of the activity profile is measured by means of up to four NaI detectors. A detailed description of the experimental setup is given in Ref. 8, and only details specific to CuBr measurement will be discussed here. The neutron-absorption properties of the bromine nuclei made tracer measurements on CuBr more difficult than the corresponding measurements on CuCl and CuI . The following neutron absorption reactions had to be taken into account:



${}^{64}\text{Cu}$ decays by positron emission and two photons with energies 511 keV are created when the positrons annihilate with electrons. This annihilation radiation is used for the determination of the concentration of ${}^{64}\text{Cu}$ tracer nuclei in the sample. The 511 keV line is relatively close to the 554 keV line originating from the decay of ${}^{82}\text{Br}$, and the NaI scintillation detectors are unable to resolve these lines. It is however possible to separate these lines by performing the measurement in coincidence mode as described in Ref. 7. The two γ rays are emitted 180° apart and it is therefore possible to distinguish the decay of the ${}^{64}\text{Cu}$ tracer nuclei by counting the 511 keV photons in coincidence. However, two additional processes give contributions to the 511 keV line even in the coincidence mode. Several γ lines with energies greater than twice 511 keV are present in the bromine spectrum and photons with these high energies can undergo pair production in which an electron positron pair is created. This process can take place in the sample itself or in the lead shielding. The positrons produced in the pair production process will annihilate with electrons and in this way contribute to the 511 keV line. Furthermore random coincidence of Compton scattered photons originating from high-energy lines can also contribute to the 511 keV line. The activity profile measured for the 511 keV line will in this way contain contributions from ${}^{64}\text{Cu}$ and ${}^{82}\text{Br}$. No substantial ${}^{64}\text{Cu}$ diffusion has taken place at room temperature and the spatial distribution of the ${}^{64}\text{Cu}$ and ${}^{82}\text{Br}$ contributions will coincide at this temperature. Cu^+ is diffused at elevated temperatures, while the Br^- ions are considered to be stationary. The total activity profile measured at elevated temperature will therefore contain a ${}^{82}\text{Br}$ contribution, which has the same shape and half width as the total profile measured at room temperature. The ${}^{82}\text{Br}$ contribution has been accounted for in the analysis of the measured activity profiles, but care was taken to make this contribution as small as possible during the irradiation of the sample. We have recently shown that the Br^- ions are diffusing with a diffusion coefficient of the order $10^{-7} \text{ cm}^2/\text{sec}$ in $\alpha\text{-CuBr}$, while no Br diffusion could be detected in the γ and β phases.¹⁰

The ${}^{82}\text{Br}$ contains several resonance absorption peaks at epithermal neutron energies and these peaks give a substantial contribution to the total neutron absorption cross section. The initial irradiations showed that the ${}^{82}\text{Br}$ contribution to the coincidence rate was about 10% at the beginning of a measurement and increasing with time. The creation of ${}^{82}\text{Br}$ nuclei was therefore minimized by irradiating the sample in a position in the reactor where the ratio of the epithermal to thermal neutron flux was as low as possible. Samples irradiated this way showed no significant ${}^{82}\text{Br}$ contribution to the coincidence rate.

The analysis of the measured activity profiles was performed as follows. The spatial distribution of radioactive nuclei at time t is related to the initial distribution at $t=0$ through the equation

$$I(x, t) = e^{-\lambda t} \int I(x', 0) P(x - x', t) dx'. \quad (1)$$

$I(x, 0)$ is the distribution measured at $t=0$, λ is the radioactive decay constant, and $P(x, t)$ is the diffusion function to be determined. In the present cylindrical geometry, the solution to the diffusion equation depends only on the coordinate x along the cylinder

$$P(x, t) = \frac{S(0)}{2\sqrt{\pi Dt}} e^{-x^2/4Dt}, \quad (2)$$

where $S(0)$ is the total source strength at $t=0$ and D is the diffusion coefficient. The activity profile is therefore at all times a function with variance

$$\sigma^2(I(x, t)) = \sigma^2(I(x, 0)) + \sigma^2(P(x, t)). \quad (3)$$

From (2) it is seen that $\sigma^2(P(x, t)) = 2Dt$ and D is therefore determined directly from the variance of the measured activity profile by the equation

$$D = \frac{1}{2t} \{ \sigma^2(I(x, t)) - \sigma^2(I(x, 0)) \}. \quad (4)$$

When mounted in the furnace the sample was first scanned at room temperature and then heated up to the temperature at which the measurement was to be performed. Heating and subsequent equilibration took about 90 min. The temperature was measured by a Chromel-Alumel thermocouple. After equilibration the sample temperature was maintained stable to better than $\pm 0.6^\circ\text{C}$. Typically 10–20 activity profiles were measured at each temperature, and the measurement of these took 1.5–5 h depending on the magnitude of the diffusion coefficient. Data analysis was performed by least-squares fitting of a Gaussian plus a linear or, in some cases, a parabolic background function to the measured profiles. No asymmetry in any of the measured profiles was observed, which shows that the time needed for scanning a profile is negligible compared to the rate of diffusion. Sample inhomogeneities caused by cracks in the sample will immediately show up in the measured profiles. The source position at $t=0$ is treated as an adjustable parameter in the determination of $\sigma^2(I(x, t))$ and the determination of D is not affected by resolution effects and the spatial extent of the source at $t=0$, because these effects cancel out according to (4).

TABLE I. Diffusion coefficients at various temperatures for Cu^+ diffusion in CuBr.

T (K)	D (cm^2/sec)	
523	$2(1) \times 10^{-8}$	γ phase
577	$2.9(6) \times 10^{-8}$	
603	$5.1(5) \times 10^{-7}$	
623	$1.8(4) \times 10^{-6}$	
645	$3.20(6) \times 10^{-6}$	
693	$2.1(1) \times 10^{-5}$	β phase
723	$2.6(1) \times 10^{-5}$	
733	$2.8(1) \times 10^{-5}$	
744	$3.2(6) \times 10^{-5}$	α phase
746	$3.1(1) \times 10^{-5}$	
749	$3.4(1) \times 10^{-5}$	
754	$3.1(1) \times 10^{-5}$	

III. RESULTS AND DISCUSSION

Activity profiles were measured for the temperature given in Table I and as an example selected activity profiles measured at 693 K are shown in Fig. 1. Plots of $\sigma^2(I(x,t))$ versus t are shown in Fig. 2. The measured tracer-diffusion coefficients for the γ phase are in good agreement with the results obtained in an earlier conventional tracer-diffusion study by Schäfer and Richter who performed measurements in the temperature range 443 to 615 K.⁹ A plot of $\log D$ versus $1000/T$ for α , β , and γ -CuBr is shown in Fig. 3. Points belonging to the γ and β phase fall on straight lines indicating that the diffusion in these phases can be described by an Arrhenius equation

$$D = D_0 e^{-E_a/k_B T}, \quad (5)$$

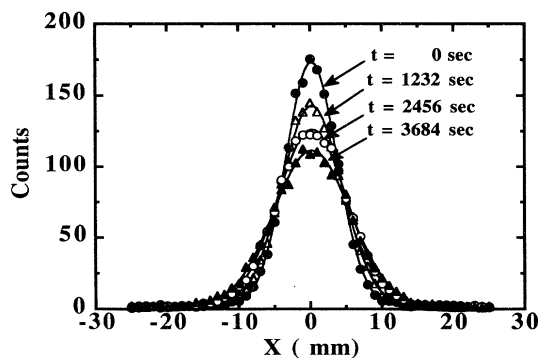


FIG. 1. Plot of selected activity profiles measured at 693 K. The profiles shown here were corrected for the decay of the ^{64}Cu nuclei. The solid curves represent a Gaussian plus a linear background fitted to the measured points.

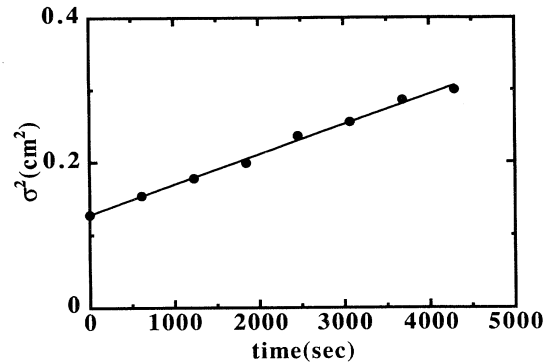


FIG. 2. Plot of $\sigma^2(I(x,t))$ versus time for activity profiles measured at 693 K.

where E_a is activation energy and k_B is Boltzmann's constant. The Arrhenius plot given by Schäfer and Richter did however show some curvature which indicates that the Cu^+ diffusion in γ -CuBr cannot be described by the Arrhenius equation over a more extended temperature range. The curvature of the Arrhenius plot might well be due to two or more concurrent diffusion processes, each with its own activation energy, and with their relative contributions changing with temperature. The activation energy for Cu^+ diffusion in CuBr is given in Table II together with the corresponding activation energies for CuCl and CuI measured by the *in situ* tracer method^{5,7,8} and Arrhenius plots for CuCl and CuI are shown for comparison in Fig. 4. The temperature interval in which α -CuBr is stable is rather narrow, and it was therefore impossible to determine an activation energy for Cu^+ diffusion in α -CuBr. CuBr has the lowest activation energy of the three copper halides in the γ phase, while the activation energies are almost equal for CuCl and CuI. It is rather surprising that CuCl and CuI have equal activation energies taking into account that the iodide ions are considerably larger than chloride ions.

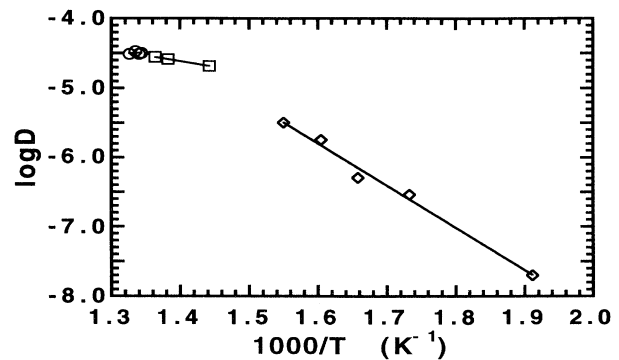


FIG. 3. Plot of $\log D$ versus $1000/T$ for CuBr. Points marked with circles, diamonds, and squares belong to the α , β , and γ phases, respectively. The points in the γ and β phase were fitted to an Arrhenius equation (solid line). D is in cm^2/sec .

TABLE II. Activation energies in eV for Cu^+ diffusion in the copper halides.

	γ phase	β phase	α phase	Ref.
CuCl	1.4(1)			8
CuBr	1.21(7)	0.324(1)		
CuI	1.30	0.91(9)	0.31	5,7

The activation energy found in β -CuBr is considerably lower than the corresponding value for β -CuI. The activation energies found in β -CuBr and α -CuI are quite similar and from Figs. 3 and 4, it is seen that the diffusion coefficient in β -CuBr is about two and four times larger than the diffusion coefficients measured in α -CuI and β -CuI, respectively.

It is rather remarkable that the change in the diffusion coefficient encountered by going from the β to the α phase is so small in the case of CuBr. For CuCl and CuI large jumps in the diffusion coefficients are observed at the structural phase transitions which is also the case for the γ - β transition in CuBr. A recent conductivity study of CuBr also shows a rather modest jump in the conductivity at the β - α transition.¹¹ The high value of the diffusion coefficient in the β phase of CuBr presumably indicates that this phase is highly disordered with the Cu^+ ions occupying both sets of tetrahedral holes in the hexagonal structure. This view is supported by thermodynamic measurements for the copper halides. The entropy changes at the γ - β transition are 7.115, 7.005, and 4.82 J/K mol, while the entropy changes during melting are 10.178, 6.725, and 9.139 J/K mol for CuCl, CuBr, and CuI, respectively.¹² The β phases in both CuCl and CuBr therefore have a higher degree of disorder than the β -CuI phase. Furthermore Nölting has shown that the specific heat increases in β -CuI and decreases in β -CuBr for increasing temperature. His explanation is that β -CuBr is formed in a state where the cations are completely disordered but the cations in β -CuI are becoming in-

creasingly disordered as the temperature is increased.¹³

Safadi *et al.*, in a recent conductivity measurement on γ -CuBr, have shown that the ionic conductivity is impurity controlled below 573 K with a transition to intrinsic Frenkel equilibria above this temperature. The activation energies were found to be 1.1 and 1.85 eV above and below 573 K, respectively, leading to a migration enthalpy of 1.1 eV and Frenkel energy of 1.50 eV. The activation energy or migration enthalpy in the β phase was found to be 0.35 eV.¹¹ These activation energies are in reasonable agreement with the values obtained in the present study.

A comparison of measured tracer-diffusion coefficients and charge diffusion coefficient calculated from conductivity measurements can, in principle, yield information about the microscopic diffusion mechanism. The charge diffusing coefficient D_q is related to the tracer-diffusion coefficient D by the relation

$$f = \frac{D}{D_q}, \quad (6)$$

where f is the Haven ratio. D_q is related to the ionic conductivity by the Nernst-Einstein equation:

$$D_q = \frac{k_B T}{n(Ze)^2} \sigma, \quad (7)$$

where k_B is the Boltzmann constant, T is the temperature in Kelvin, n and Z are the number density and charge of the diffusing ion and e is the electronic charge. Table III contains calculated values of f for the three copper halides at selected temperatures in the α , β , and γ phases. The Haven ratio f is smaller than or equal to one in the case that the charge and mass transport are due to the same diffusion process. As seen in Table III, f is however greater than one for all the copper halide phases except for α and β phase CuBr. Schäfgen and Richtering made the same observation in their study of γ -CuBr and they proposed that an additional transport process which does not carry charge is taking place in γ -CuBr.⁹ Two copper ions are interchanging sites in the proposed diffusion process via intermediate jumps to an empty tetrahedral copper site and no net charge is therefore moved in the process. The zinc-blende structure is especially suited for this type of diffusion process because only half of the tetrahedral sites are occupied by copper ions. A full investigation of the diffusion processes in the copper halides would however require that tracer-diffusion and conductivity measurements are made on the same samples. In addition, an eventual contribution to the diffusion process from grain-boundary diffusion should also be taken into consideration which would require knowledge about the grain-size distribution in the sample.

A full understanding of the role of ionic size, mass, and polarizability for the ionic diffusion in and the dynamics of copper halides will require molecular-dynamic simula-

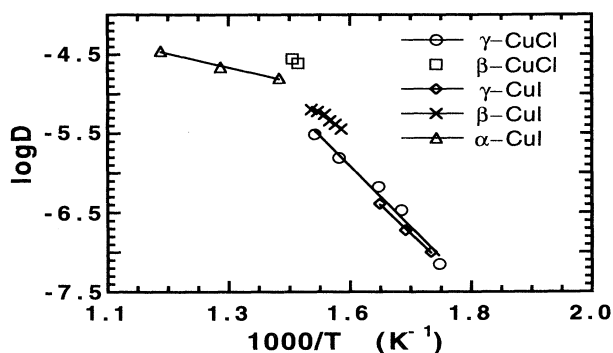


FIG. 4. Arrhenius plot of tracer-diffusion coefficients for CuCl and CuI measured by the *in situ* tracer-diffusion technique. D is in cm^2/sec . Data for CuCl are taken from Ref. 8, while the CuI data are from Refs. 5 and 7.

TABLE III. Conductivities, diffusion coefficients, and Haven ratios for the copper halides. Conductivity data are from Wagner and Wagner, Ref. 13 (CuCl and CuI) and from Safadi, Riess, and Tuller, Ref. 11 (CuBr).

	T K	σ ($\Omega^{-1} \text{cm}^{-1}$)	D (cm^2/sec)	D_q (cm^2/sec)	f	
CuCl	624	1.45×10^{-2}	$6.7(4) \times 10^{-7}$	1.93×10^{-7}	3.5	
CuBr	623	6.54×10^{-2}	$1.80(4) \times 10^{-6}$	1.05×10^{-6}	1.7	γ phase
CuI	605	7.30×10^{-3}	$1.9(4) \times 10^{-7}$	1.34×10^{-7}	1.4	
CuBr	723	1.21	$2.6(1) \times 10^{-5}$	2.18×10^{-5}	0.9	β phase
CuI	666	7.76×10^{-2}	$5.53(4) \times 10^{-6}$	1.58×10^{-6}	3.5	
CuBr	750	2.26	$3.4(1) \times 10^{-5}$	4.32×10^{-5}	0.8	α phase
CuI	763	0.1	$2.2(4) \times 10^{-5}$	2.386×10^{-6}	9.2	

tions of all the phases for each compound. The results of our tracer-diffusion studies will, in conjunction with thermodynamic quantities, be used as input parameters for an evaluation of the validity of the interatomic potential used in molecular-dynamics simulations of the copper halides.

ACKNOWLEDGMENTS

The authors would like to thank Lars-Erik Karlson and Martin Grönros for technical assistance during data collection, Jens Berthelsen for help in sample preparation, and Ingvar Ebbsjö for enlightening discussions.

¹T. Maatsui and J. B. Wagner, Jr., in *Solid Electrolytes, General Principles, Characterization, Materials, Applications*, edited by P. Hagenmueller and W. van Gool (Academic, New York, 1978), p. 237.

²Y. Yude, H. Boysen, and H. Schulz, *Z. Kristallogr.* **191**, 79 (1990).

³S. Hoshino, *J. Phys. Soc. Jpn.* **7**, 560 (1952).

⁴T. Kudo and K. Fueki, *Solid State Ionics*, (Kondansha, Tokyo, 1990), p. 122.

⁵R. Dejus, K. Sköld, and B. Granéli, *Solid State Ionics* **1**, 327 (1980).

⁶P. Vashishta and A. Rahman, in *Fast Ion Transport in Solids, Electrodes, and Electrolytes*, edited by P. Vashishta, J. N. Mundy, and G. K. Shenoy (North-Holland, Amsterdam, 1979), p. 527.

⁷J. X. M. Z. Johansson, K. Sköld, and J.-E. Jørgensen, *Solid State Ionics* **50**, 247 (1992).

⁸J.-E. Jørgensen, J. X. M. Z. Johansson, and K. Sköld, *J. Solid State Chem.* **98**, 263 (1992).

⁹H.-P. Schäfgen and R. Richtering, *Ber. Bunsenges. Phys. Chem.* **88**, 401 (1984).

¹⁰J. X. M. Z. Johansson, K. Sköld, and J.-E. Jørgensen, *Solid State Ionics* **59**, 297 (1993).

¹¹R. Safadi, I. Riess, and H. L. Tuller, *Solid State Ionics* **57**, 125 (1992).

¹²I. Barin, *Thermochemical Data of Pure Substances* (VCH Verlagsgesellschaft, Stuttgart, 1993), Part I.

¹³J. Nölting, J. Troe, and D. Rein, *Nachr. Akad. Wiss. Göttingen, Math Phys. Kl.* **2**, 31 (1969).

¹⁴J. B. Wagner and C. Wagner, *J. Chem. Phys.* **26**, 1597 (1957).